# Quantum Langevin equations for semiconductor light-emitting devices and the photon statistics at a low-injection level

Hiroshi Fujisaki* and Akira Shimizu†
*Institute of Physics, University of Tokyo, 3-8-1 Komaba, Tokyo 153-8902, Japan*
(Received 25 April 1997; revised manuscript received 17 December 1997)

From the microscopic quantum Langevin equations (QLEs) we derive the effective semiconductor QLEs and the associated noise correlations which are valid at a low-injection level and in real devices. Applying the semiconductor QLEs to semiconductor light-emitting devices (LEDs), we obtain a formula for the Fano factor of photons that gives the photon-number statistics as a function of the pump statistics and several parameters of LEDs. Key ingredients are nonradiative processes, carrier-number dependence of the radiative and nonradiative lifetimes, and multimodeness of LEDs. The formula is applicable to the actual cases where the quantum efficiency $\eta$ differs from the differential quantum efficiency $\eta_d$, whereas previous theories implicitly assumed $\eta = \eta_d$. It is also applicable to the cases where photons in each mode of the cavity are emitted and/or detected inhomogeneously. When $\eta_d < \eta$ at a running point, in particular, our formula predicts that even a Poissonian pump can produce sub-Poissonian light. This mechanism for generation of sub-Poissonian light is completely different from those of previous theories, which assumed sub-Poissonian statistics for the current injected into the active layers of LEDs. Our results agree with recent experiments. We also discuss frequency dependence of the photon statistics. [S1050-2947(98)09504-3]

PACS number(s): 42.50.Lc

## I. INTRODUCTION

There has been much research on quantum noise in light-emitting devices (LEDs) since the celebrated work of Shawllow and Townes [1]. We here consider the quantum noise in semiconductor LEDs. This subject was first studied by Haug and Haken [2], who derived from a microscopic model useful formulas for the first- and second-order optical coherence of LEDs.

Recently, much attention has been paid to sub-Poissonian light (SPL), which has lower intensity fluctuations than the standard quantum limit [3], of various LEDs [4–14]. The mechanism for generation of SPL in LEDs is quite different from that of squeezed light in nonlinear crystals [15]. The latter mechanism is well understood as a Bogoliuvov transformation of a coherent state into a squeezed state of light [16]. The former mechanism, on the other hand, is often described by the Langevin theory of lasers [3,17–21]. Previous studies on SPL in LEDs assumed that only a single mode or a few modes of photons are excited [4,6,14]. When the injection level is lowered, however, many modes of photons become relevant, and we must consider all of them. Simple theories for such a case were reported in Refs. [5,7]. However, they are *too* simplified so that they cannot explain recent experiments by Hirano, Kuga (HK), and co-workers [9–11], who demonstrated that the experimental results at a low-injection level (LIL) disagree with the predictions of the simplified theories. The disagreement appears when the quantum efficiency $\eta$ differs from the differential quantum efficiency $\eta_d$. HK [9] suggested that nonradiative processes might be responsible for the disagreement.

In this paper, to resolve the discrepancy between the previous theories and the experiments, we theoretically investigate the quantum noise in LEDs *at a low-injection level* [22]. To this end, we extend the Langevin-equation method of Chow, Koch, and Sargent [21] to treat the case where many photon modes are excited in an LED. From the microscopic quantum Langevin equations (QLEs) and the associated noise correlations, we derive the semiconductor QLEs and the noise correlations at the LIL. An important assumption is that the photon-absorption and emission rates are much smaller than the photon-escape rate from a ''cavity.''[1] In the experiment [12], it has been reported that $\eta_d/\eta > 2$ in low-injection regions, whereas $\eta \simeq \eta_d$ in high-injection regions. The difference between $\eta$ and $\eta_d$ is, in our theory, attributed to nonradiative processes and the carrier-number dependence of lifetimes. They always exist in real LEDs, and become particularly important in low-injection regions. In contrast, we can easily show that the previous simplified theories [4–7] always give $\eta = \eta_d$. Hence our theory is a minimal one to simulate real LEDs. A formula for the photon Fano factor [6] is derived. It gives the photon-number statistics as a function of the pump statistics, measuring frequency, $\eta$, $\eta_d$, and some factors arising from *multimodeness* of LEDs. Simplified formulas are derived for homogeneous cases, in which photons in each mode of the cavity are emitted and detected homogeneously, and for inhomogeneous cases, in which they are emitted and/or detected inhomogeneously. Using these formulas, we discuss the condition for generation of SPL in an LED. Our results agree with the experimental results.

*Electronic address: fujisaki@ASone.c.u-tokyo.ac.jp
†Electronic address: shmz@ASone.c.u-tokyo.ac.jp

[1]The validity of this assumption with the meaning of the ''cavity'' will be explained in the Appendix.

 

The paper is organized as follows. In Sec. II, we derive the semiconductor QLEs and the noise correlations at the LIL. In Sec. III, the semiconductor QLEs are used to derive a formula for the photon Fano factor. In Sec. IV, we examine the formula in various cases, and compare our theory with recent experiments [9–12]. In Sec. V, we summarize the paper.

## II. DERIVATION OF QUANTUM LANGEVIN EQUATIONS AND THE NOISE CORRELATIONS AT A LOW-INJECTION LEVEL

### A. Microscopic Langevin equations of an LED

Chow *et al.* [21] discussed the case where a *single mode* is excited among many-photon modes of a cavity. Since we are mainly interested in the photon statistics of LEDs at the LIL, we extend their method to treat *many modes* of photons. The total Hamiltonian $\mathcal{H}_{\rm tot}$ (which describes multimode photons in the cavity and carriers in the active layer of an LED) is written as

$$\mathcal{H}_{\rm tot}=\mathcal{H}_{\text{multi-ph}}+\mathcal{H}_{\rm carrier}+\mathcal{H}_{\rm dipole}+\mathcal{H}_{\text{many-body}}+\mathcal{H}_{\rm baths}+\mathcal{H}_{\text{baths-sys}}, \tag{1}$$

$$\mathcal{H}_{\text{multi-ph}}=\sum_l \hbar\nu_l a_l^\dagger a_l, \tag{2}$$

$$\mathcal{H}_{\rm carrier}=\sum_{\mathbf{k}}\left[\left(\epsilon_{\rm g}^0+\frac{\hbar^2k^2}{2m_e}\right)c_{\mathbf{k}}^\dagger c_{\mathbf{k}}+\frac{\hbar^2k^2}{2m_h}d_{-\mathbf{k}}^\dagger d_{-\mathbf{k}}\right], \tag{3}$$

$$\mathcal{H}_{\rm dipole}=\sum_{l,\mathbf{k}}\hbar(g_{l,\mathbf{k}}^0 d_{-\mathbf{k}}^\dagger c_{\mathbf{k}}^\dagger a_l+\text{H.c.}), \tag{4}$$

where $\mathcal{H}_{\text{multi-ph}}$ is the Hamiltonian of the multimode photons, $a_l$ is the annihilation operator for the photons in mode $l$, and $\nu_l$ is the field oscillation frequency in mode $l$. The Hamiltonian of the electrons and holes in the active layer is $\mathcal{H}_{\rm carrier}$. The annihilation operators of the electron and hole of wave vector $\mathbf{k}$ are $c_{\mathbf{k}}$ and $d_{-\mathbf{k}}$, respectively, $m_e$ and $m_h$ are the electron and hole effective masses, respectively, and $\epsilon_g^0$ is the bare band-gap energy. The interaction among the carriers and the photons is represented by $\mathcal{H}_{\rm dipole}$ in the dipole approximation, with $g_{l,\mathbf{k}}^0$ being the bare coupling constants, and H.c. means Hermite conjugate. Note that here we consider only a direct radiative transition; however, in real devices there are other processes, and we will include them when necessary. The many-body interaction between the carriers is represented by $\mathcal{H}_{\text{many-body}}$, the Hamiltonian of baths (or environments) by $\mathcal{H}_{\rm baths}$, and the interaction between the baths and the system (the carriers and photons) by $\mathcal{H}_{\text{baths-sys}}$.

To obtain QLEs, we start by making a mean-field approximation for $\mathcal{H}_{\text{many-body}}$, and consequently $\epsilon_g^0$ and $g_{\mathbf{k},l}^0$ are renormalized (see, e.g., Chap. 4 of Ref. [21]). The renormalized parameters are denoted by $\epsilon_g$ and $g_{l,\mathbf{k}}$.

We then eliminate $\mathcal{H}_{\rm baths}+\mathcal{H}_{\text{baths-sys}}$ by using the Markov approximation [3,16–21]. As a result, the fluctuation and dissipation terms appear in the equations of motion. The generalized Einstein relation [16–18,20,21] gives the relation between the fluctuation and dissipation terms as follows:

$$2D_{\mu\nu}=\frac{d}{dt}\langle A_\mu A_\nu\rangle-\langle D_\mu A_\nu\rangle-\langle A_\mu D_\nu\rangle, \tag{5}$$

where $2D_{\mu\nu}$ is a diffusion coefficient, $A_\mu$ is a system variable, and $D_\mu$ is a dissipation term in Langevin equations, i.e., $\dot{A}_\mu=D_\mu+F_\mu, \langle F_\mu(t)F_\nu(t')\rangle=2D_{\mu\nu}\delta(t-t')$. The brackets mean the ensemble average for fluctuations.

We finally obtain the following microscopic QLEs, which describe LEDs in a microscopic scale, for the dipole operator $\sigma_{\mathbf{k}}=d_{-\mathbf{k}}c_{\mathbf{k}}e^{i\nu_l t}$, for the electric field operator $A_l(t)=a_l(t)e^{i\nu_l t}$, and for the electron occupation probability in $\mathbf{k}$ space $n_{e\mathbf{k}}=c_{\mathbf{k}}^\dagger c_{\mathbf{k}}$,

$$\frac{d}{dt}\sigma_{\mathbf{k}}=-(\gamma+i\omega_{\mathbf{k}}-i\nu_l)\sigma_{\mathbf{k}}+i\sum_{l'}g_{l',\mathbf{k}}A_{l'}(n_{e\,\mathbf{k}}+n_{h\,\mathbf{k}}-1)+F_{\sigma\mathbf{k}}, \tag{6}$$

$$\frac{d}{dt}A_l=-\left(\frac{\kappa_l^0}{2}+i(\Omega_l-\nu_l)\right)A_l-i\sum_{\mathbf{k}}g_{l,\mathbf{k}}^*\sigma_{\mathbf{k}}+F_l, \tag{7}$$

$$\frac{d}{dt}n_{e\mathbf{k}}=P_{e\mathbf{k}}(1-n_{e\mathbf{k}})-\frac{n_{e\mathbf{k}}}{\tau_{\rm nr}}+\sum_l(ig_{l,\mathbf{k}}^*A_l^\dagger\sigma_{\mathbf{k}}+\text{H.c.})+F_{e\mathbf{k}}, \tag{8}$$

where $\gamma$ is the dipole decay (dephasing) rate, $\hbar\omega_{\mathbf{k}}\equiv\epsilon_g+\hbar^2k^2/2m_e+\hbar^2k^2/2m_h$ is the transition energy, and $F_{\sigma\mathbf{k}}$ is the fluctuation operator for the dipole. The hole occupation probability in $\mathbf{k}$ space is $n_{h\mathbf{k}}\equiv d_{-\mathbf{k}}^\dagger d_{-\mathbf{k}}$. The photon escape rate from the cavity is $\kappa_l^0=\nu_l/Q_l$, where $Q_l$ is the $Q$ factor of the cavity, $\Omega_l$ is the passive-cavity frequency, and $F_l$ is the fluctuation operator for the electric field. The pump rate due to a current injection or optical pumping is $P_{e\mathbf{k}}(1-n_{e\mathbf{k}})$, where the factor $(1-n_{e\mathbf{k}})$ represents the pump blocking [21]. Note that a lifetime of nonradiative decay $\tau_{\rm nr}$ has been introduced in Eq. (8). As discussed later, the existence of nonradiative processes is, in our model, a necessary condition for the difference between the quantum efficiency and the differential quantum efficiency to occur. The other condition is that the lifetime of radiative processes or that of nonradiative ones varies with $n_c$. [See Eqs. (66)–(68).] Nonradiative processes might be modeled by the capture of carriers at a trapping level in an LED; however, we only need that $\tau_{\rm nr}$ is an implicit function of $n_c$. These terms of pump and nonradiative decay have been phenomenologically introduced. The fluctuation operator for the electron number is $F_{e\mathbf{k}}$.

### B. Adiabatic approximation

To derive more useful forms for later discussion, we use the adiabatic approximation [19,23], and approximate the solution of Eq. (6) by

$$\sigma_{\mathbf{k}}\simeq\frac{i\Sigma_{l'}g_{l',\mathbf{k}}A_{l'}(n_{e\mathbf{k}}+n_{h\mathbf{k}}-1)+F_{\sigma\mathbf{k}}}{\gamma+i\omega_{\mathbf{k}}-i\nu_l}. \tag{9}$$

Substituting Eq. (9) into Eq. (7), we find

$$\dot{A}_l = -[\kappa_l^0/2 + i(\Omega_l - \nu_l)]A_l + \sum_{l'} G_{ll'}A_{l'} + F_l + F_{\sigma,l}, \tag{10}$$

where $G_{ll'}$ is a ''gain matrix'';

$$G_{ll'} \equiv \sum_{\mathbf{k}} g^*_{l,\mathbf{k}} g_{l',\mathbf{k}} \mathcal{D}_{l,\mathbf{k}}(n_{e\mathbf{k}} + n_{h\mathbf{k}} - 1), \tag{11}$$

where $\mathcal{D}_{l,\mathbf{k}}$ is a complex Lorentzian; $\mathcal{D}_{l,\mathbf{k}} \equiv 1/[\gamma + i(\omega_{\mathbf{k}} - \nu_l)]$. A fluctuation operator $F_{\sigma,l}(t)$ has been defined by

$$F_{\sigma,l} \equiv -i \sum_{\mathbf{k}} g^*_{l,\mathbf{k}} \mathcal{D}_{l,\mathbf{k}} F_{\sigma\mathbf{k}}, \tag{12}$$

which is associated with the coupling between the carriers and photons.

From Eq. (10), we also find the QLE for the photon-number operator $n_l \equiv A_l^\dagger A_l$,

$$\frac{d}{dt} n_l = -\kappa_l^0 n_l + \sum_{l'} [G_{ll'} A_l^\dagger A_{l'} + \text{H.c.}] + [(F^\dagger_{\sigma,l} + F^\dagger_l) A_l + \text{H.c.}]. \tag{13}$$

Substituting Eq. (9) into Eq. (8), we also find the QLE for the total electron number $n_c \equiv \Sigma_{\mathbf{k}} n_{e\mathbf{k}}$,

$$\frac{d}{dt} n_{\text{c}} = \sum_{\mathbf{k}} P_{e\mathbf{k}}(1 - n_{e\mathbf{k}}) - \frac{n_c}{\tau_{\text{nr}}} - \sum_{l,l'} [G_{ll'} A_l^\dagger A_{l'} + \text{H.c.}] + \sum_{\mathbf{k}} F_{e\mathbf{k}} - \sum_l [A_l^\dagger F_{\sigma,l} + \text{H.c.}]. \tag{14}$$

### C. Microscopic noise correlations of an LED

To discuss the statistical properties of light emitted from LEDs, we must determine the noise correlations. Hereafter we assume that the correlations between different modes of the photons and those between different wave numbers of carriers can be neglected [19], i.e.,

$$\langle A_l^\dagger(t) A_{l'}(t) \rangle \simeq \langle n_l \rangle \delta_{ll'}, \tag{15}$$

$$\langle \sigma^\dagger_{\mathbf{k}}(t) \sigma_{\mathbf{k}'}(t) \rangle \simeq \langle n_{e\mathbf{k}} n_{h\mathbf{k}} \rangle \delta_{\mathbf{k},\mathbf{k}'}, \tag{16}$$

$$\langle \sigma_{\mathbf{k}}(t) \sigma^\dagger_{\mathbf{k}'}(t) \rangle \simeq \langle (1 - n_{e\mathbf{k}})(1 - n_{h\mathbf{k}}) \rangle \delta_{\mathbf{k},\mathbf{k}'}, \tag{17}$$

$$\langle n_{e\mathbf{k}}(t) n_{e\mathbf{k}'}(t) \rangle \simeq \langle n_{e\mathbf{k}} \rangle \delta_{\mathbf{k},\mathbf{k}'}. \tag{18}$$

We can then calculate the noise correlations, which are consistent with the QLEs (6)–(8), using Eq. (5),

$$\langle F^\dagger_{\sigma\mathbf{k}}(t) F_{\sigma\mathbf{k}'}(t') \rangle \simeq 2\gamma \langle n_{e\mathbf{k}} n_{h\mathbf{k}} \rangle \delta_{\mathbf{k},\mathbf{k}'} \delta(t - t'), \tag{19}$$

$$\langle F_{\sigma\mathbf{k}}(t) F^\dagger_{\sigma\mathbf{k}'}(t') \rangle \simeq 2\gamma \langle (1 - n_{e\mathbf{k}})(1 - n_{h\mathbf{k}}) \rangle \times \delta_{\mathbf{k},\mathbf{k}'} \delta(t - t'), \tag{20}$$

$$\langle F_l^\dagger(t) F_{l'}(t') \rangle \simeq \kappa_l^0 \overline{n(\nu_l)} \delta_{ll'} \delta(t - t'), \tag{21}$$

$$\langle F_l(t) F^\dagger_{l'}(t') \rangle \simeq \kappa_l^0 [\overline{n(\nu_l)} + 1] \delta_{ll'} \delta(t - t'), \tag{22}$$

$$\langle F_{e\mathbf{k}}(t) F_{e\mathbf{k}'}(t') \rangle = [\langle P_{e\mathbf{k}}(1 - n_{e\mathbf{k}}) \rangle + \langle n_{e\mathbf{k}}/\tau_{\text{nr}} \rangle] \times \delta_{\mathbf{k},\mathbf{k}'} \delta(t - t'), \tag{23}$$

where $\overline{n(\nu_l)}$ is the number of thermal photons in mode $l$ in the cavity. We have used, in Eqs. (19) and (20), the quasi-equilibrium conditions [21]

$$2\gamma \langle n_{e\mathbf{k}} n_{h\mathbf{k}} \rangle \gg \frac{d}{dt} \langle n_{e\mathbf{k}} n_{h\mathbf{k}} \rangle, \tag{24}$$

$$2\gamma \langle (1 - n_{e\mathbf{k}})(1 - n_{h\mathbf{k}}) \rangle \gg \frac{d}{dt} \langle (1 - n_{e\mathbf{k}})(1 - n_{h\mathbf{k}}) \rangle. \tag{25}$$

We can also calculate the correlations of $F_{\sigma,l}$;

$$\langle F^\dagger_{\sigma,l}(t) F_{\sigma,l}(t') \rangle = \langle R_{\text{sp},l} \rangle \delta(t - t'), \tag{26}$$

$$\langle F_{\sigma,l}(t) F^\dagger_{\sigma,l}(t') \rangle = \langle R_{\text{abs},l} \rangle \delta(t - t'), \tag{27}$$

where $R_{\text{sp},l}$ ($R_{\text{abs},l}$) denotes the spontaneous emission rate into photon mode $l$ (the absorption rate of photon mode $l$);

$$R_{\text{sp},l} \equiv \frac{n_{\text{c}}}{\tau_{\text{r},l}} \equiv \frac{2}{\gamma} \sum_{\mathbf{k}} |g_{l,\mathbf{k}}|^2 \mathcal{L}_{l,\mathbf{k}} n_{e\mathbf{k}} n_{h\mathbf{k}}, \tag{28}$$

$$R_{\text{abs},l} \equiv \frac{2}{\gamma} \sum_{\mathbf{k}} |g_{l,\mathbf{k}}|^2 \mathcal{L}_{l,\mathbf{k}} (1 - n_{e\mathbf{k}})(1 - n_{h\mathbf{k}}). \tag{29}$$

We have used Eqs. (19) and (20), and defined $\tau_{\text{r},l}$ as a radiative lifetime of the carriers into mode $l$. The (dimensionless) Lorentzian line-shape function $\mathcal{L}_{l,\mathbf{k}}$ is $\mathcal{L}_{l,\mathbf{k}} \equiv \gamma^2/[\gamma^2 + (\omega_{\mathbf{k}} - \nu_l)^2]$.

At this stage, we have the following QLEs:

$$\frac{d}{dt} n_l = -\kappa_l n_l + [(F^\dagger_{\sigma,l} + F^\dagger_l) A_l + \text{H.c.}], \tag{30}$$

$$\frac{d}{dt} n_c = \sum_{\mathbf{k}} P_{e\mathbf{k}}(1 - n_{e\mathbf{k}}) - \frac{n_c}{\tau_{\text{nr}}} - \sum_l (R_{\text{sp},l} - R_{\text{abs},l}) n_l + \sum_{\mathbf{k}} F_{e\mathbf{k}} - \sum_l [A_l^\dagger F_{\sigma,l} + \text{H.c.}], \tag{31}$$

where we have used

$$G_{ll} + G^*_{ll} = R_{\text{sp},l} - R_{\text{abs},l}, \tag{32}$$

and defined the renormalized photon escape rate

$$\kappa_l = \kappa_l^0 - R_{\text{sp},l} + R_{\text{abs},l}. \tag{33}$$

### D. Semiconductor Langevin equations and the noise correlations for an LED at a low-injection level

In what follows, we assume[2]

$$R_{\mathrm{sp},l}, R_{\mathrm{abs},l} \ll \kappa_l^0. \tag{34}$$

From Eqs. (30) and (34), the QLE for $n_l$ at the LIL becomes

$$\frac{d}{dt} n_l = -\kappa_l^0 n_l + R_{\mathrm{sp},l} + F_{n,l}, \tag{35}$$

where we have defined a fluctuation operator,

$$F_{n,l} \equiv [(F_{\sigma,l}^\dagger + F_l^\dagger) A_l + \mathrm{H.c.}] - [\kappa_l^0 \overline{n(\nu_l)} + R_{\mathrm{sp},l}]. \tag{36}$$

The right-hand side is averaged to be zero because the noises, $F_{n,l}$ and $F_{\sigma,l}$, have the Markovian property: $\langle F_l^\dagger A_l + \mathrm{H.c.}\rangle = \kappa_l^0 \overline{n(\nu_l)}$ and $\langle F_{\sigma,l}^\dagger A_l + \mathrm{H.c.}\rangle = R_{\mathrm{sp},l}$.

From Eqs. (34) and (35), the steady-state value of the photon number becomes

$$(n_l)_{\mathrm{s.s.}} \simeq R_{\mathrm{sp},l}/\kappa_l^0 \ll 1, \tag{37}$$

i.e., the photon number in each mode is quite small. On the other hand, from Eqs. (31), (34), and (37), the QLE for $n_{\mathrm{c}}$ at the LIL becomes

$$\frac{d}{dt} n_c = P - \frac{n_c}{\tau_{\mathrm{r}}} - \frac{n_c}{\tau_{\mathrm{nr}}} + F_c, \tag{38}$$

where $P \equiv \Sigma_{\mathbf{k}} P_{e\mathbf{k}}(1 - n_{e\mathbf{k}})$ is the total pump rate, and

$$\frac{1}{\tau_{\mathrm{r}}} \equiv \frac{\Sigma_l R_{\mathrm{sp},l}}{n_c} \equiv \sum_l \frac{1}{\tau_{\mathrm{r},l}} \tag{39}$$

is the radiative decay rate ($\tau_{\mathrm{r}}$ is the radiative lifetime of carriers). The fluctuation operator for the total electron number $F_c$ is denoted by

$$F_c \equiv \sum_l [-(A_l^\dagger F_{\sigma,l} + \mathrm{H.c.}) + R_{\mathrm{sp},l}] + \sum_{\mathbf{k}} F_{e\mathbf{k}}. \tag{40}$$

Note that the lifetimes ($\tau_{\mathrm{r},l}$ and $\tau_{\mathrm{r}}$) are carrier-number $n_c$ dependent because $R_{\mathrm{sp},l}$ is an implicit function of $n_c$.

We thus obtain the final forms of the semiconductor QLEs at the LIL as follows:

$$\frac{d}{dt} n_c = P - \frac{n_c}{\tau_{\mathrm{r}}} - \frac{n_c}{\tau_{\mathrm{nr}}} + \Gamma_P + \Gamma_{\mathrm{r}} + \Gamma_{\mathrm{nr}}, \tag{41}$$

$$\frac{d}{dt} n_l = -\kappa_l^0 n_l + \frac{n_c}{\tau_{\mathrm{r},l}} + F_{\kappa,l} + F_{\mathrm{r},l}, \tag{42}$$

where the noise operators $F_{n,l}, F_c$ have been divided into new ones, $\Gamma_{\mathrm{r}}, F_{\mathrm{r},l}, \Gamma_{\mathrm{nr}}, \Gamma_P, F_{\kappa,l}$. They are given by

$$\Gamma_{\mathrm{r}} \equiv \sum_l [-(A_l^\dagger F_{\sigma,l} + \mathrm{H.c.}) + R_{\mathrm{sp},l}], \tag{43}$$

$$F_{\mathrm{r},l} \equiv A_l^\dagger F_{\sigma,l} + \mathrm{H.c.} - R_{\mathrm{sp},l}, \tag{44}$$

$$\Gamma_{\mathrm{nr}} + \Gamma_{\mathrm{P}} \equiv \sum_{\mathbf{k}} F_{e\mathbf{k}}, \tag{45}$$

$$F_{\kappa,l} \simeq A_l^\dagger F_l + F_l^\dagger A_l, \tag{46}$$

where we have neglected the number of thermal photons, $\overline{n(\nu_l)}$, since this is the case in usual experiments. These noise operators ($\Gamma_{\mathrm{r}}, F_{\mathrm{r},l}, \Gamma_{\mathrm{nr}}, \Gamma_P, F_{\kappa,l}$) are associated with the radiative decay of carriers, the conversion from carriers to photons, the nonradiative decay of carriers, the (intrinsic) pump fluctuation, and the photon escape from the cavity, respectively. The mean values of the noises are defined to be zero, of course.

From above, the noise correlation for $\Gamma_{\mathrm{r}}$ can be calculated as

$$\begin{aligned}
\langle \Gamma_{\mathrm{r}}(t)\Gamma_{\mathrm{r}}(t')\rangle &\simeq \sum_l [\langle A_{c,l}^\dagger(t) A_{c,l}(t')\rangle \langle F_{\sigma,l}(t) F_{\sigma,l}^\dagger(t')\rangle \\
&\quad + \langle A_{c,l}(t) A_{c,l}^\dagger(t')\rangle \langle F_{\sigma,l}^\dagger(t) F_{\sigma,l}(t')\rangle] \\
&= \sum_l [\langle R_{\mathrm{sp},l} + R_{\mathrm{abs},l}\rangle \langle n_l\rangle + \langle R_{\mathrm{sp},l}\rangle] \delta(t-t') \\
&\simeq \sum_l \langle R_{\mathrm{sp},l}\rangle \delta(t-t') = \left\langle \frac{n_c}{\tau_{\mathrm{r}}} \right\rangle \delta(t-t'),
\end{aligned} \tag{47}$$

where, as done in Eq. (15), we have neglected, in the first and second lines, the correlations between different modes. We also have assumed the following:

$$\Gamma_{\mathrm{r}} \simeq \sum_l [-(A_{c,l}^\dagger F_{\sigma,l} + \mathrm{H.c.})],$$

where $A_{c,l}^\dagger$ is an operator uncorrelated with $F_{\sigma,l}$ [24]. Thus the property of fluctuations, $\langle \Gamma_{\mathrm{r}}\rangle = 0$, still holds. Equations (26) and (27) have also been used in the third line of Eq. (47), and Eqs. (34), (37), and (39) in the fourth line of Eq. (47).

Similarly we obtain

$$\langle \Gamma_{\mathrm{r}}(t) F_{\mathrm{r},l}(t')\rangle = -\left\langle \frac{n_c}{\tau_{\mathrm{r},l}} \right\rangle \delta(t-t'), \tag{48}$$

$$\langle F_{\mathrm{r},l}(t) F_{\mathrm{r},l'}(t')\rangle = \left\langle \frac{n_c}{\tau_{\mathrm{r},l}} \right\rangle \delta_{ll'} \delta(t-t'), \tag{49}$$

$$\langle \Gamma_{\mathrm{nr}}(t)\Gamma_{\mathrm{nr}}(t')\rangle = \left\langle \frac{n_c}{\tau_{\mathrm{nr}}} \right\rangle \delta(t-t'), \tag{50}$$

$$\langle \Gamma_P(t)\Gamma_P(t')\rangle = \langle P\rangle \delta(t-t'), \tag{51}$$

where we have divided the correlation $\langle \Gamma_{\mathrm{nr}}(t)\Gamma_{\mathrm{nr}}(t')\rangle + \langle \Gamma_P(t)\Gamma_P(t')\rangle$ into two parts: one is the correlation of the nonradiative processes, and the other that of the pump. These semiconductor QLEs, Eqs. (41) and (42), and the noise cor-

[2]Inequality (34), at first sight, might look rather strange. We therefore explain its validity *at the LIL* in the Appendix.

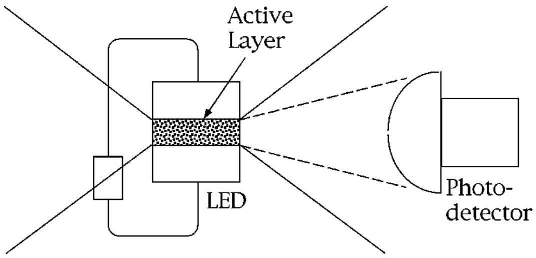


FIG. 1. Definition of the $\xi_l$. Photons of mode $l$ are emitted into the region between the solid lines. The photodetector can detect only some region (denoted by the one between the dashed lines) of the photons because its surface area is limited, and the quantum efficiency $\eta$ of the detector is less than 1. $\xi_l$ is the probability that a photon of mode $l$ is detected by the detector. It increases as the surface area and/or $\eta$ do.

relations (47)–(51) were just assumed by us [22,25]. Yamanishi and Lee [5] also assumed similar ones; however, they did not include nonradiative processes.

Furthermore, we focus on the total photon flux, $N$, which can be detected at the PD surface. To this end, we must find two relations. One is the relation between the photon number in the cavity and the photon flux from the cavity. The other is the relation between the photon flux from the cavity and the photon flux detected at the PD surface. The input-output formalism [3,20] gives the first relation as

$$V_l = \kappa_l^0 n_l - F_{\kappa,l}, \tag{52}$$

where $V_l$ is the photon flux of mode $l$ from the cavity. We next model the second relation using the argument of a beam splitter [20]. The relation between the mean flux of $N$ and that of $V_l$ is given by

$$\langle N\rangle = \sum_l \xi_l \langle V_l\rangle \equiv \beta_0 \sum_l \langle V_l\rangle \equiv \beta_0 \langle V\rangle, \tag{53}$$

where $\xi_l$ is a ''transmission coefficient'' of mode $l$ (see Fig. 1), $\beta_0$ is the transfer efficiency [5], and $V \equiv \Sigma_l V_l$ is the total photon flux from the cavity. The relation between the flux correlation of $N$ and that of $V_l$ is given by

$$\langle |\Delta \tilde{N}(\Omega)|^2\rangle = \sum_l \xi_l (1-\xi_l)\langle \tilde{V}_l(\Omega)\rangle + \sum_{l,l'} \xi_l \xi_{l'} \langle \Delta \tilde{V}_l(\Omega) \Delta \tilde{V}_{l'}(\Omega)\rangle, \tag{54}$$

where $\tilde{N}(\Omega)$ and $\tilde{V}_l(\Omega)$ denote Fourier components of $N$ and $V_l$, respectively.

## III. CALCULATION OF THE PHOTON FANO FACTOR

In this section, we calculate the Fano factor of photons [6] which denotes the normalized fluctuation of the photon number detected at the PD surface. Following the standard small-signal analysis used in Refs. [4,5,7,14], we expand the radiative and nonradiative lifetimes, $\tau_{\mathrm{r},l}[n_c]$, $\tau_{\mathrm{r}}[n_c]$, and $\tau_{\mathrm{nr}}[n_c]$, to linear order in $\Delta n_c \equiv n_c - n_{c0}$:

$$\tau_{\mathrm{r},l}[n_c] = (\tau_{\mathrm{r},l})_0 \left(1 - K_{\mathrm{r},l} \frac{\Delta n_c}{n_{c0}}\right), \tag{55}$$

$$\tau_{\mathrm{r}}[n_c] = \tau_{\mathrm{r}0} \left(1 - K_{\mathrm{r}} \frac{\Delta n_c}{n_{c0}}\right), \tag{56}$$

$$\tau_{\mathrm{nr}}[n_c] = \tau_{\mathrm{nr}0} \left(1 + K_{\mathrm{nr}} \frac{\Delta n_c}{n_{c0}}\right), \tag{57}$$

$$\frac{1}{\tau_{\mathrm{r}0}} \equiv \sum_l \frac{1}{(\tau_{\mathrm{r},l})_0}, \tag{58}$$

$$K_{\mathrm{r}} = \sum_l \frac{\tau_{\mathrm{r}0}}{(\tau_{\mathrm{r},l})_0} K_{\mathrm{r},l}, \tag{59}$$

where quantities with the subscript 0 denote the average values at a running point, $P = P_0$. Sensitivity of lifetimes to the carrier-number fluctuations $\Delta n_c$ is represented by $K_{\mathrm{r},l}$, $K_{\mathrm{r}}$, and $K_{\mathrm{nr}}$. Though $K_{\mathrm{r}}$ is usually positive, it is not always the case, as we will discuss in the next section.

Linearizing Eqs. (41), (42), and (52) in terms of $\Delta n_c$, $\Delta n_l \equiv n_l - (n_l)_0$, $\Delta P \equiv P - P_0$, and $\Delta V_l \equiv V_l - (V_l)_0$, and substituting Eqs. (55) and (57) into them, we obtain

$$\frac{d}{dt}\Delta n_c = \Delta P - \frac{\Delta n_c}{\tau''} + \Gamma_P + \Gamma_{\mathrm{r}} + \Gamma_{\mathrm{nr}}, \tag{60}$$

$$\frac{d}{dt}\Delta n_l = -\kappa_l^0 \Delta n_l + \frac{\Delta n_c}{\tau'_{\mathrm{r},l}} + F_{\kappa,l} + F_{\mathrm{r},l}, \tag{61}$$

$$\Delta V_l = \kappa_l^0 \Delta n_l - F_{\kappa,l}, \tag{62}$$

where we have used the following equilibrium conditions:

$$P_0 = n_{c0}\left(\frac{1}{\tau_{\mathrm{r}0}} + \frac{1}{\tau_{\mathrm{nr}0}}\right),$$

$$\sum_l \kappa_l^0 (n_l)_0 = \sum_l \frac{n_{c0}}{(\tau_{\mathrm{r},l})_0} = \frac{n_{c0}}{\tau_{\mathrm{r}0}} = \sum_l V_{l0} = V_0 = \frac{P_0}{1 + (\tau_{\mathrm{r}0}/\tau_{\mathrm{nr}0})}, \tag{63}$$

and introduced the effective lifetimes defined as

$$\tau'_{\mathrm{r}} \equiv \frac{\tau_{\mathrm{r}0}}{1+K_{\mathrm{r}}}, \quad \tau'_{\mathrm{r},l} \equiv \frac{(\tau_{\mathrm{r},l})_0}{1+K_{\mathrm{r},l}}, \quad \tau'_{\mathrm{nr}} \equiv \frac{\tau_{\mathrm{nr}0}}{1-K_{\mathrm{nr}}}, \tag{64}$$

$$\frac{1}{\tau''} \equiv \frac{1}{\tau'_{\mathrm{r}}} + \frac{1}{\tau'_{\mathrm{nr}}}. \tag{65}$$

Dropping the noise terms in Eqs. (60)–(62), and using Eq. (53), we calculate the quantum efficiency $\eta$ and the differential quantum efficiency $\eta_d$ as

$$\eta \equiv \frac{N_0}{P_0} = \frac{\beta_0/\tau_{\mathrm{r}0}}{(1/\tau_{\mathrm{r}0} + 1/\tau_{\mathrm{nr}0})} = \frac{\beta_0}{1+\epsilon_0}, \tag{66}$$

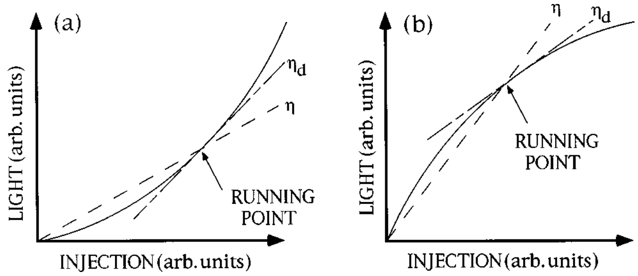


FIG. 2. Typical IL (injection-light) characteristics of LEDs are shown by the solid lines. The quantum efficiency $\eta$ is the slope of the straight line (represented by the dashed line) connecting the origin and the running point, whereas the differential quantum efficiency $\eta_d$ is the slope of the tangential line (chain line) at the running point.

$$\eta_d \equiv \left. \frac{\Delta \tilde{N}(\Omega)}{\Delta \tilde{P}(\Omega)} \right|_{\Omega \to 0} = \frac{\beta_0 / \tau_{\rm r}'}{(1/\tau_{\rm r}' + 1/\tau_{\rm nr}')} = \frac{\beta_0}{1+\epsilon'}, \tag{67}$$

where

$$\epsilon_0 \equiv \frac{\tau_{\rm r0}}{\tau_{\rm nr0}}, \quad \epsilon' \equiv \frac{\tau_{\rm r}'}{\tau_{\rm nr}'} = \frac{1-K_{\rm nr}}{1+K_{\rm r}} \epsilon_0 . \tag{68}$$

These efficiencies ($\eta$ and $\eta_d$) are illustrated in Fig. 2.

Note that the difference between $\eta$ and $\eta_d$, which was measured to be large (e.g., $\eta_d / \eta > 2$ at the LIL [12]), cannot be explained by the previous theories which assumed $\tau_{\rm nr0} = \infty$ [4–6] or $K_{\rm r} = K_{\rm nr} = 0$ [7]. In this sense, our model is a *minimal* one that simulates real LEDs.

Hereafter we assume that $\Omega \ll \kappa_l^0$ ($\sim 10^{12}$ Hz), which is well satisfied in usual experimental conditions. Then the response of the output photon flux to the modulation of the pump is calculated as

$$\left| \frac{\Delta \tilde{N}(\Omega)}{\Delta \tilde{P}(\Omega)} \right| = \frac{\eta_d}{\sqrt{1+\Omega^2 \tau''^2}} . \tag{69}$$

Hence $1/\tau''$ is understood as a cutoff frequency. It is seen that the nonradiative processes push the cutoff to the higher frequency [see Eq. (65)].

On the other hand, the photon flux correlation between mode $l$ and $m$ is calculated using Eqs. (60)–(62) as

$$\begin{aligned} \langle \Delta \tilde{V}_l^*(\Omega) \Delta \tilde{V}_m(\Omega) \rangle = & \frac{\tau''}{\tau_{{\rm r},l}'} \frac{\tau''}{\tau_{{\rm r},m}'} \frac{\langle |\Delta \tilde{P}_{\rm tot}|^2 \rangle + \langle |\tilde{\Gamma}_{\rm r}|^2 \rangle + \langle |\tilde{\Gamma}_{\rm nr}|^2 \rangle}{1+(\Omega \tau'')^2} \\ & + \frac{\tau''}{\tau_{{\rm r},l}'} \frac{\langle \tilde{\Gamma}_{\rm r}^* \tilde{F}_{{\rm r},m} \rangle}{1-i\Omega\tau''} + \frac{\tau''}{\tau_{{\rm r},m}'} \frac{\langle \tilde{\Gamma}_{\rm r}^* \tilde{F}_{{\rm r},l} \rangle}{1+i\Omega\tau''} \\ & + \langle \tilde{F}_{{\rm r},l}^* \tilde{F}_{{\rm r},m} \rangle , \end{aligned} \tag{70}$$

where a total pump noise $\Delta \tilde{P}_{\rm tot}$ has been defined as

$$\Delta \tilde{P}_{\rm tot}(\Omega) \equiv \Delta \tilde{P}(\Omega) + \tilde{\Gamma}_P(\Omega),$$

which consists of the modulation $\Delta \tilde{P}(\Omega)$ and the intrinsic pump noise $\tilde{\Gamma}_P(\Omega)$. Note that the latter noise can be suppressed by inelastic scattering in conductors [4,8–10,26].

To see the physical meaning of Eq. (70), let us introduce the Fano factor of the pump electrons (or excitons) $W_e$ and that of the photons detected at the PD surface $W_{\rm ph}$, which are defined by

$$W_e(\Omega) \equiv \frac{\langle |\Delta \tilde{P}_{\rm tot}(\Omega)|^2 \rangle}{P_0 T}, \tag{71}$$

$$W_{\rm ph}(\Omega) \equiv \frac{\langle |\Delta \tilde{N}(\Omega)|^2 \rangle}{N_0 T}, \tag{72}$$

where $T$ is the Fourier-integral time. We transform Eqs. (47)–(51) into the Fourier components:

$$\begin{aligned} \langle \tilde{F}_{\rm r}^*(\Omega) \tilde{F}_{\rm r}(\Omega) \rangle = \langle \tilde{\Gamma}_{\rm r}^*(\Omega) \tilde{\Gamma}_{\rm r}(\Omega) \rangle = \frac{1}{\epsilon_0} \langle \tilde{\Gamma}_{\rm nr}^*(\Omega) \tilde{\Gamma}_{\rm nr}(\Omega) \rangle \\ = - \langle \tilde{\Gamma}_{\rm r}^*(\Omega) \tilde{F}_{\rm r}(\Omega) \rangle = \frac{n_{c0}}{\tau_{\rm r0}} T = V_0 T = \frac{P_0 T}{1+\epsilon_0} . \end{aligned} \tag{73}$$

Substituting Eqs. (70) and (73) into Eq. (54), and dividing by $N_0 T$, we finally obtain

$$W_{\rm ph}(\Omega) = 1 - \frac{2\eta_d \zeta_1}{1+(\Omega\tau'')^2} + \frac{\eta_d^2}{\eta} \frac{1+W_e(\Omega)}{1+(\Omega\tau'')^2} \zeta_2 , \tag{74}$$

where we have used Eqs. (53), (63), (66)–(68), and defined the following:

$$\zeta_1 \equiv \sum_{l,m} \frac{\tau_{\rm r}'}{\tau_{{\rm r},l}'} \frac{\tau_{\rm r0}}{(\tau_{{\rm r},m})_0} \frac{\xi_l}{\beta_0} \frac{\xi_m}{\beta_0}, \tag{75}$$

$$\zeta_2 \equiv \left[ \sum_l \frac{\tau_{\rm r}'}{\tau_{{\rm r},l}'} \frac{\xi_l}{\beta_0} \right]^2, \tag{76}$$

which represent effects due to multimodeness of LEDs, and the consequences are discussed below. Note also that $\zeta_1 \leq 1, \zeta_2 \leq 1$.

Equation (74) is our main result which gives the Fano factor of the photons detected at the PD surface as a function of the Fano factor of the pump, measuring frequency, and several parameters ($\eta, \eta_d, \zeta_1, \zeta_2$, and $\tau''$). Note that $1/\tau''$ becomes a cutoff frequency of the Fano factor as well as that of the modulation [see Eq. (69)].

## IV. DISCUSSION

### A. Low-frequency limit

Let us examine Eq. (74) in two cases, $\Omega = 0$ and $\Omega > 0$, separately. We first discuss the low-frequency limit. This case is applicable to the most experiments, because they are usually performed at the frequency which is lower than any other relevant frequencies. Setting $\Omega \to 0$, we obtain

$$W_{\rm ph}(0) = 1 - 2\eta_d \zeta_1 + \frac{\eta_d^2}{\eta} [1+W_e(0)] \zeta_2 . \tag{77}$$

There are several cases where this expression becomes simpler.

#### 1. The case where photons are emitted and detected homogeneously (the homogeneous case)

(h-1). When photons in each mode are emitted and detected *homogeneously*, i.e., when $K_{\mathrm{r},l}=K_{\mathrm{r}}=\mathrm{const}$ and $\xi_l=\beta_0=\mathrm{const}$, we have $\zeta_1=\zeta_2=1$, hence

$$W_{\mathrm{ph}}(0)=1-2\eta_d+\frac{\eta_d^2}{\eta}[1+W_e(0)]. \tag{78}$$

This is the formula that we have derived elsewhere [25]. We have implicitly assumed this property (h-1) there, and this is a natural choice unless one considers a situation such that inhomogeneity due to, e.g., cavity-QED effects becomes important.

(h-2). In addition to (h-1), when the nonradiative processes do not exist and/or the carrier-number dependence of lifetimes cancels to be zero, i.e., $\tau_{\mathrm{nr}0}\to\infty$ and/or $K_{\mathrm{r}}+K_{\mathrm{nr}}=0$, we have $\eta=\eta_d$ and the IL (injection-light) characteristics become straight. Hence, from Eq. (78), we obtain

$$\begin{aligned}W_{\mathrm{ph}}(0)&=1-2\eta+\eta[1+W_e(0)]\\&=1-\eta+\eta W_e(0).\end{aligned} \tag{79}$$

This is just the previous formula which is frequently used in the literature [6–9,13].

#### 2. The case where photons are emitted and/or detected inhomogeneously (the inhomogeneous case)

Note that in the homogeneous case the factors $\zeta_1$ and $\zeta_2$ do not appear in the expressions for $W_{\mathrm{ph}}$ [Eqs. (78) and (79)]. On the other hand, they appear when emission and/or detection efficiencies are different among different modes. We call this general case the ''inhomogeneous case.'' To investigate this case, let us consider a simple case where $K_{\mathrm{r},l}=0$ and $K_{\mathrm{nr}}\neq 0$. In this case, $\zeta_1=\zeta_2\equiv\zeta$, where

$$\zeta\equiv\left[\sum_l\frac{\tau_{\mathrm{r}0}}{(\tau_{\mathrm{r},l})_0}\frac{\xi_l}{\beta_0}\right]^2. \tag{80}$$

Hence, from Eq. (77), we obtain

$$W_{\mathrm{ph}}(0)=1-2\eta_d\zeta+\frac{\eta_d^2\zeta}{\eta}[1+W_e(0)]. \tag{81}$$

Compared with Eq. (78), we see that $\eta$ and $\eta_d$ are effectively multiplied by $\zeta$ in Eq. (81). However, this does not mean that $\zeta$ could be absorbed in $\eta$ and $\eta_d$, because they are already defined by Eqs. (66) and (67), respectively. Any redefinition would lead to disagreement with the observed IL characteristics.

#### 3. Condition for generation of sub-Poissonian light

As another illustration of our result, we next discuss the condition for generation of sub-Poissonian light (SPL) ($W_{\mathrm{ph}}<1$) with a Poissonian pump ($W_e=1$). For simplicity, we hereafter consider the case (h-1) [Eq. (78)], because many LEDs seem to be categorized in this case. From Eq. (78), we obtain

$$0<\eta_d<\eta \tag{82}$$

as the condition. It can be intuitively understood that the flatter the IL characteristics, the duller the sensitivity of the LED to the pump fluctuation. Hence, if IL characteristics are like Fig. 2(b), then *even a Poissonian pump* ($W_e=1$) *can produce sub-Poissonian light*. Note that this mechanism is completely different from those of Refs. [7,13,27], because the authors of [7,13,27] eventually make the current noise injected to the active layers *below Poissonian*. On the other hand, the condition (82) is equivalent to

$$K_{\mathrm{r}}+K_{\mathrm{nr}}<0, \tag{83}$$

where we have used Eqs. (66)–(68). For simplicity, we here take $K_{\mathrm{nr}}=0$, and find below what is needed for $K_{\mathrm{r}}<0$.

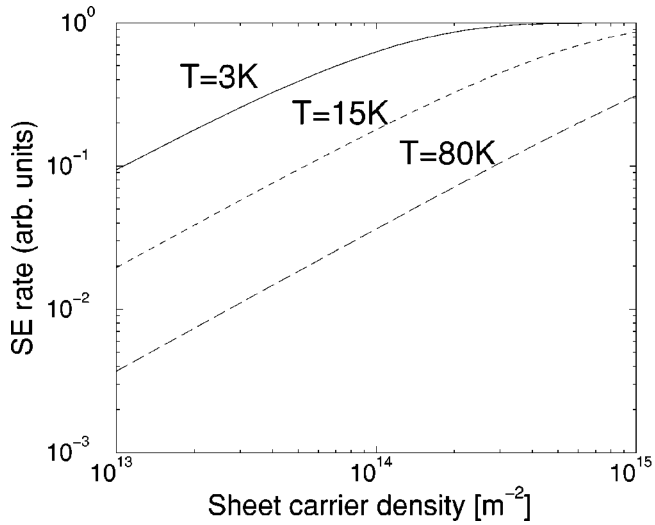


FIG. 3. The spontaneous emission (SE) rate as a function of carrier population in a doped-quantum-well structure in a microcavity. Three curves correspond to different temperatures: $T=$ 80 K (bottom), $T=$ 15 K (middle), and $T=$ 3 K (top).

The spontaneous emission (SE) rate $n_c/\tau_{\mathrm{r}}$ may be expressed approximately as $n_c/\tau_{\mathrm{r}}\propto(n_c)^p$, where $p$ is a constant. We therefore have $K_{\mathrm{r}}\simeq p-1$ from Eq. (56). It is well known [21] that $p\simeq 1$ ($p\simeq 2$) in high- (low-) injection regions for SE processes of free carriers. For exciton recombination, we have $p\simeq 1$ at the LIL. Thus we usually have nonnegative values of $K_{\mathrm{r}}$. Making use of cavity-QED effects, however, we can obtain *negative* values of $K_{\mathrm{r}}$. This is illustrated in Fig. 3 for a $p$-doped quantum well structure in a microcavity, where we have assumed the following: the conduction band is parabolic, the effective electron mass is 0.1 times the free electron mass, the doping level is high, and the cavity-QED effects prohibit SE except at the band edge.

It is seen that $K_{\mathrm{r}}$ becomes negative for the sheet carrier density $\gtrsim 10^{14}$ $\mathrm{m}^{-2}$ when temperatures are low enough (maybe below 3 K). In this case, we obtain $\eta_d<\eta$ [see Eqs. (66)–(68)], and even a super-Poissonian pump can produce SPL. Exciton recombination with cavity-QED effects would work better, which will be discussed elsewhere. It has been

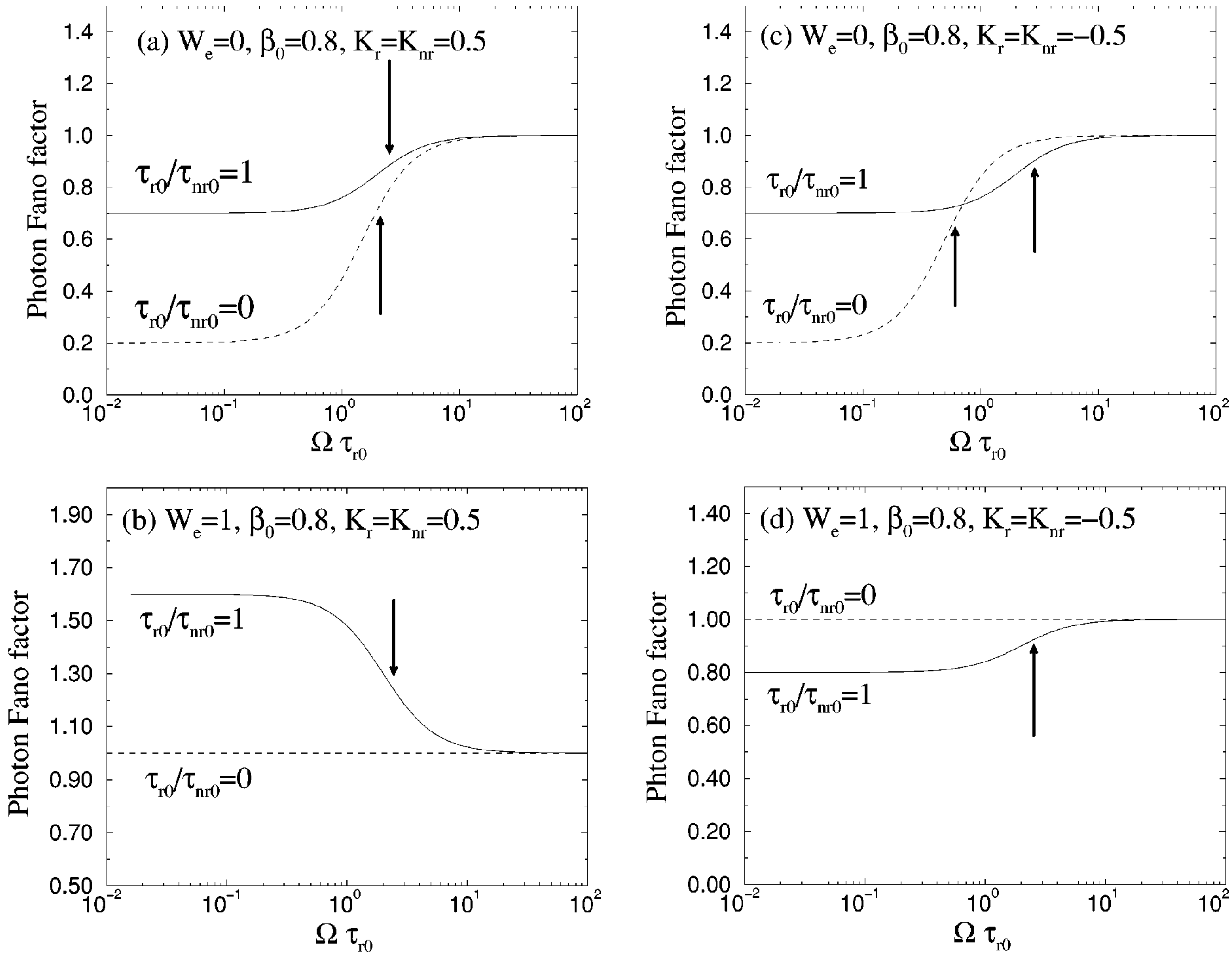


FIG. 4. The photon Fano factors are plotted as functions of frequency $\Omega$ (in units of $1/\tau_{r0}$). (a) and (b) represent the cases where $K_r = K_{nr} = 0.5$. (c) and (d) represent the cases where $K_r = K_{nr} = -0.5$. The pump noise level is assumed to be zero ($W_e = 0$) and the Poissonian level ($W_e = 1$) in (a),(c) and (b),(d), respectively. In each figure, the solid and dashed lines represent the cases where the nonradiative recombination is significant ($\tau_{r0}/\tau_{nr0} = 1$) and absent ($\tau_{r0}/\tau_{nr0} = 0$), respectively. The cutoff frequencies are indicated by vertical arrows.

therefore shown that our formula (74) is useful to find the condition for generation of SPL, or, of course, other quantum states of light.

### B. Finite-frequency cases

Let us turn to the finite frequency cases. For simplicity, here we use Eq. (74) with property (h-1), i.e., $\zeta_1 = \zeta_2 = 1$, and assume the case where $K_r = K_{nr}$ in Fig. 4. The solid lines (dashed lines) in Fig. 4 represent the cases when nonradiative processes exist (do not exist).

#### *1. When $K_r = K_{nr} = 0.5$*

The noiseless ($W_e = 0$) and Poissonian ($W_e = 1$) pumps are denoted by Figs. 4(a) and 4(b), respectively. When $\tau_{nr0} = \infty$ (dashed lines), we recover the results similar to those of Yamanishi and Lee [5]. We also see that the cutoff frequency (indicated by a vertical arrow) for $\tau_{nr0} \neq \infty$ becomes higher than that for $\tau_{nr0} = \infty$ [Fig. 4(a)].

#### *2. When $K_r = K_{nr} = -0.5$*

The noiseless ($W_e = 0$) and Poissonian ($W_e = 1$) pumps are denoted by Figs. 4(c) and 4(d), respectively. We find that the existence of nonradiative processes gives smaller $W_{ph}$ in some frequency region [Fig. 4(c)] or in the entire frequency range [Fig. 4(d)]. In particular, Fig. 4(d) shows that the Poissonian pumping can produce SPL in a wide frequency range. Figure 4(c) also shows that the cutoff frequency for $\tau_{nr0} \neq \infty$ becomes higher than that for $\tau_{nr0} = \infty$ as well as Fig. 4(a) does.

It might be difficult, however, to observe these features experimentally, because they would not appear up to $1/\tau_{r0} \sim 1$ GHz. (Recently the photon Fano factor of LEDs has been measured up to 40 MHz [12].)

### C. Comparison with the experimental results

Hirano and Kuga [9] reported that the previous formula (79) disagrees with their experimental data in low-frequency regions: They measured the following ratio,

$$\frac{W_{ph}(W_e = 0)}{W_{ph}(W_e = 1)} \equiv r, \tag{84}$$

and obtained that $r < 1 - \eta$, whereas Eq. (79) gives $r = 1 - \eta$. Since the measuring frequency $\Omega_{meas}$ is low enough,

TABLE I. The experimental values of $\eta, \eta_d, r$ and the theoretical values of $r$ (after Ref. [11]).

| $\eta$ (Expt.) | $\eta_d$ (Expt.) | $r$ (Expt.) | $r$ [Eq. (85)] | $r=1-\eta$ |
|---|---|---|---|---|
| 0.067 | 0.090 | 0.90 | 0.89 | 0.93 |
| 0.104 | 0.125 | 0.84 | 0.86 | 0.90 |
| 0.150 | 0.175 | 0.81 | 0.81 | 0.85 |

i.e., $\Omega_{\rm meas} \sim 10$ MHz$\ll 1/\tau'' \sim 1$ GHz, and their LEDs seem to be categorized in the homogeneous case (h-1), we can use Eq. (78) to analyze their results. Our formula (78) gives

$$r = \frac{1-2\eta_d + \eta_d^2/\eta}{1-2\eta_d + 2\eta_d^2/\eta}. \tag{85}$$

When $\eta_d > \eta$ (which is usually the case in low-injection regions [9–12]), our theory gives $r < 1-\eta$, in agreement with the experimental results. Furthermore, Hirano *et al.* [11] recently confirmed that Eq. (85) agrees with their experimental data (see Table I). It is seen that the values of the previous theory ($r=1-\eta$) are larger than the experimental values, whereas the values of Eq. (85) are closer to them. It also has been shown that, when $W_e=1$, $W_{\rm ph}$ *itself* is larger than 1 [11]. This fact also supports our formula (78) because it gives, when $W_e=1$ and $\eta_d>\eta$, $W_{\rm ph}=1-2\eta_d+2\eta_d^2/\eta>1$, and their LEDs also have the property $\eta_d>\eta$ [9,11].

On the other hand, a simple argument [11,28] leads to

$$W_{\rm ph}(0) = 1-\eta + \frac{\eta_d^2}{\eta} W_e(0). \tag{86}$$

Since $|\eta-\eta_d|$ is small in Table I, the difference between this formula and Eq. (78) is within the experimental error and is not detectable. Further experimental studies are needed to observe the difference.

## V. SUMMARY

From the microscopic QLEs (6)–(8), the associated noise correlations (19)–(23), and the assumption (34), we have derived the effective semiconductor QLEs (41), (42), and the associated noise correlations (47)–(51). The assumption (34) is valid at a low-injection level and in real devices as explained in the Appendix. Applying the semiconductor QLEs to semiconductor LEDs, we obtain a formula (74) for the Fano factor of photons. It gives the photon-number statistics as a function of the pump statistics and several parameters of LEDs, which are defined by Eqs. (65)–(68), (75), and (76). Key ingredients are nonradiative processes, carrier-number dependence of lifetimes, and multimodeness of LEDs. The formula is applicable to the actual cases where the quantum efficiency $\eta$ differs from the differential quantum efficiency $\eta_d$, whereas the previous theories [4–7] turn out to give $\eta=\eta_d$. It is also applicable to cases where photons in each mode of the cavity are emitted and/or detected inhomogeneously. When $\eta_d<\eta$ at the running point, in particular, our formula predicts that even a Poissonian pump can produce sub-Poissonian light (see Sec. IV A 3). This mechanism for generation of sub-Poissonian light is completely different from those of the previous theories, which assumed sub-Poissonian statistics for the current injected into the active layers of LEDs. It was shown that our results agree with recent experiments by Hirano, Kuga, and co-workers [9–12]. We have also found that, in finite frequency regions, nonradiative processes sometimes give better results (smaller $W_{\rm ph}$ and/or a higher cutoff frequency). These will deserve further theoretical and experimental research of quantum aspects of light emitted from LEDs.

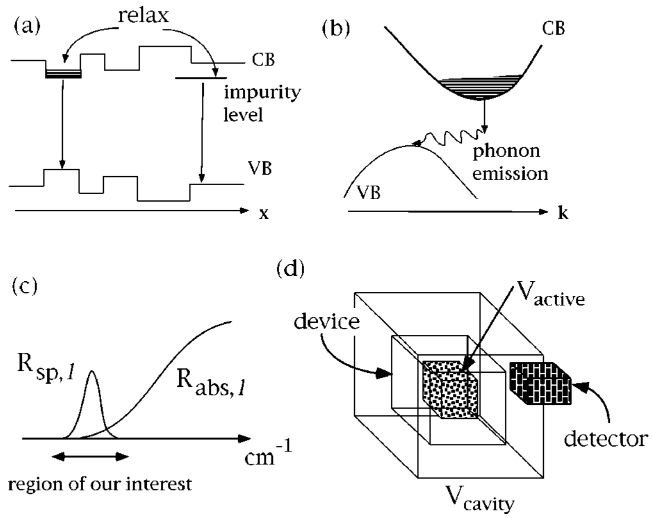


FIG. 5. (a) A schematic band diagram of real LEDs at the LIL, (b) the Stokes shift [CB (VB) represents the conduction (valence) band], (c) the absorption and emission profiles at the LIL, and (d) the active layer, the device (LED), and the "cavity."

## ACKNOWLEDGMENTS

We would like to thank T. Hirano and T. Kuga for drawing our attention to this problem. We are also grateful to M. Yamanishi, Y. Lee, G. Shinozaki, and J. Abe for fruitful discussions. This work has been supported by the Core Research for Evolutional Science and Technology (CREST) of the Japan Science and Technology Corporation (JST), and by Grants-in-Aid for Scientific Research on Priority Areas from the Ministry of Education, Science and Culture.

## APPENDIX: VALIDITY OF INEQUALITY (34)

We here show that inequality (34), $R_{{\rm sp},l}, R_{{\rm abs},l} \ll \kappa_l^0$, holds for LEDs at a low-injection level (LIL). At the LIL, pumped carriers first relax to lower-energy states which are formed by impurities, defects, spatial randomness, and so on, and then recombine to radiate photons [Fig. 5(a)]. Within the energy region of our interest, where photons are emitted, we thus have $R_{{\rm sp},l} \sim R_{{\rm abs},l}$. In addition, in real devices, there exists a Stokes shift [Fig. 5(b)] which makes, at low temperatures, $R_{{\rm abs},l}$ even smaller. Hence we have the absorption and emission profiles such as Fig. 5(c).

We now proceed to compare $R_{{\rm sp(abs)},l}$ with $\kappa_l^0$. In Eqs. (28) and (29), $|g_{l,\mathbf{k}}|^2$ is proportional to $1/V_{\rm cavity}$ ($V_{\rm cavity}$ is the volume of a cavity), and $\Sigma_{\mathbf{k}}$ is to the volume of the active layer $V_{\rm active}$, hence we have $R_{{\rm sp(abs)},l} \propto V_{\rm active}/V_{\rm cavity}$. In the analysis of *laser diodes* (LDs), it is customary to take $V_{\mathrm{active}} \simeq V_{\mathrm{cavity}}$, because LDS are made so that the lasing modes are confined in the active layer. In this case, we usually have $R_{\mathrm{abs},l}/c \sim 10^4\ \mathrm{cm}^{-1} \gg \kappa_l^0/c \sim 10^2\ \mathrm{cm}^{-1}$ ($c$ is the velocity of light), thus we cannot obtain the inequality (34). In the case of LEDs, on the other hand, they are usually designed in such a way that the reflection coefficients on the boundary surfaces are small, hence most modes of photons of our interest are not confined in the layer. In this case, it is natural to take the ''cavity'' volume as big as a cube on which the detector's surface is located [Fig. 5(d)]. Then $\kappa_l^0$ can be estimated as $1/\kappa_l^0 \simeq (V_{\mathrm{cavity}})^{1/3}/c + Q t_{\mathrm{device}}$, where $t_{\mathrm{device}}$ is a time for photons to traverse the device. Since $Q$ and $t_{\mathrm{device}}$ are small for LEDs, we have $\kappa_l^0 \simeq c/(V_{\mathrm{cavity}})^{1/3}$. Therefore, noting that $R_{\mathrm{abs},l} \propto 1/V_{\mathrm{cavity}}$ and $\kappa_l^0 \propto 1/(V_{\mathrm{cavity}})^{1/3}$, we can have the relation $R_{\mathrm{abs},l} \ll \kappa_l^0$, if we take $V_{\mathrm{cavity}}$ big enough. Thus we obtain inequality (34) for the case of LEDs at the LIL.


[1] A. L. Shawllow and C. H. Townes, Phys. Rev. **112**, 1940 (1958).

[2] H. Haug, Z. Phys. **200**, 57 (1967); H. Haug and H. Haken, *ibid.* **204**, 262 (1967).

[3] C. W. Gardiner, *Quantum Noise* (Springer-Verlag, Berlin, 1991).

[4] Y. Yamamoto, S. Machida, and O. Nilsson, Phys. Rev. A **34**, 4025 (1986); Y. Yamamoto and S. Machida, *ibid.* **35**, 5114 (1987).

[5] M. Yamanishi and Y. Lee, Phys. Rev. A **48**, 2534 (1993); M. Yamanishi, Prog. Quantum Electron. **19**, 1 (1994).

[6] M. C. Teich and B. E. A. Saleh, Prog. Opt. **26**, 1 (1988).

[7] G. Björk, Phys. Rev. A **45**, 8259 (1992).

[8] P. R. Tapster, J. G. Rarity, and J. S. Satchel, Europhys. Lett. **4**, 293 (1987).

[9] T. Hirano and T. Kuga, IEEE J. Quantum Electron. **31**, 2236 (1995).

[10] G. Shinozaki, T. Hirano, T. Kuga, and M. Yamanishi (unpublished); G. Shinozaki, J. Abe, T. Hirano, T. Kuga, and M. Yamanishi, Jpn. J. Appl. Phys., Part 1 **36**, 6350 (1997).

[11] T. Hirano, G. Shinozaki, J. Abe, and T. Kuga, Prog. Cryst. Growth Charact. Mater. **33**, 339 (1996).

[12] G. Shinozaki and J. Abe (unpublished).

[13] E. Goobar, A. Karlsson, G. Björk, and P.-J. Rigole, Phys. Rev. Lett. **70**, 437 (1993).

[14] F. Marin, A. Bramati, E. Giacobino, T.-C. Zhang, J.-Ph. Poizat, J.-F. Roch, and P. Grangier, Phys. Rev. Lett. **75**, 4606 (1995).

[15] R. E. Slusher, L. W. Hollberg, B. Yurke, J. C. Mertz, and J. F. Valley, Phys. Rev. Lett. **54**, 2409 (1985).

[16] P. Meystre and M. Sargent III, *Elements of Quantum Optics*, 2nd ed. (Springer-Verlag, Berlin, 1991).

[17] W. H. Louisell, *Quantum Statistical Properties of Radiation* (John Wiley & Sons, New York, 1973).

[18] M. Sargent III, M. O. Scully, and W. E. Lamb, Jr., *Laser Physics* (Addison-Wesley Publishing Co., Reading, MA, 1974).

[19] H. Haken, *Synergetics — An Introduction*, 2nd ed. (Springer-Verlag, Berlin, 1978); see, in particular, Sec. 8.1-8.6.

[20] D. F. Walls and G. J. Milburn, *Quantum Optics* (Springer-Verlag, Berlin, 1994).

[21] W. W. Chow, S. W. Koch, and M. Sargent III, *Semiconductor-Laser Physics* (Springer-Verlag, Berlin, 1994).

[22] A part of this work was briefly reported in H. Fujisaki and A. Shimizu, J. Phys. Soc. Jpn. **66**, 34 (1997).

[23] For the adiabatic approximation in the master-equation approach, see, e.g., C. W. Gardiner and A. Eschmann, Phys. Rev. A **51**, 4982 (1995).

[24] See Problem 20-2 in Ref. [18].

[25] H. Fujisaki and A. Shimizu (unpublished).

[26] A. Shimizu and M. Ueda, Phys. Rev. Lett. **69**, 1403 (1992); M. Ueda and A. Shimizu, J. Phys. Soc. Jpn. **62**, 2994 (1993).

[27] M. Yamanishi, K. Watanabe, N. Jikutani, and M. Ueda, Phys. Rev. Lett. **76**, 3432 (1996); J. Abe, G. Shinozaki, T. Hirano, T. Kuga, and M. Yamanishi, J. Opt. Soc. Am. B **14**, 1295 (1997).

[28] A. Shimizu (unpublished).